Hindawi
Geofluids
Volume 2020, Article ID 8878179, 13 pages
https://doi.org/10.1155/2020/8878179

Research Article

Failure Behavior of Hot-Dry-Rock (HDR) in Enhanced Geothermal Systems: Macro to Micro Scale Effects

Hongwei Zhang,[1,2] **Zhijun Wan**,[3] **and Derek Elsworth**[2]

[1]*School of Energy and Mining Engineering, China University of Mining & Technology, Beijing 100089, China*
[2]*Department of Energy and Mineral Engineering, EMS Energy Institute, and G3 Center, The Pennsylvania State University, University Park, PA 16802, USA*
[3]*Key Laboratory of Deep Coal Resource Mining (CUMT), Ministry of Education of China, School of Mines, China University of Mining & Technology, Xuzhou 221116, China*

Correspondence should be addressed to Zhijun Wan; zhjwan@163.com and Derek Elsworth; elsworth@psu.edu

Received 19 June 2020; Revised 9 July 2020; Accepted 26 July 2020; Published 21 September 2020

Academic Editor: Qian Yin

Evaluations of the mechanical properties and failure modes of granite at high temperatures are important issues for underground projects such as enhanced geothermal systems and nuclear waste disposal. This paper presents the results of laboratory experiments that investigated the physico-mechanical failure behavior of granites at high temperatures. The results allowed several important conclusions to be drawn. Both the uniaxial compressive strength (UCS) and tangent modulus decrease with increasing temperature. Specifically, the UCS-temperature curve can be divided into three sections: a section (20-200°C) where UCS shows a slight decrease, a section (200-300°C) where the UCS decreases significantly, and a third section (300-500°C) where the rate of UCS decrease stabilizes. However, in the entire temperature range from 20 to 500°C, the tangent modulus decreases exponentially. The number of acoustic emission (AE) counts decrease and the counts occur less frequently at higher temperatures. Individual grains are surrounded by a large number of microcracks at 200°C and the crack length increased significantly when heating to 300°C. Specifically, the length of micro-cracks in the granite at 300 °C could be 10 times longer okthan that at 200°C. Quenching or injecting cold water into HDRs would further weaken the rock and induce thermal damage to the rock structure. The strength of rock would be further quench-weakened by 10%, 20% and 30% at 200°C, 300°C and 500°C, respectively. Therefore, in Enhanced/Engineered Geothermal Systems (EGS), quenching is much more destructive than normal thermal stress.

1. Introduction

Rocks hosting Enhanced/Engineered Geothermal Systems (EGS) are subjected to elevated temperatures (e.g., heating during heat restoring) or reduced temperatures (e.g., quenching during hydraulic fracturing), as shown in Figure 1. These thermal treatments typically result in modifications to the mechanical properties of the rock and the response of the couple THMC processes [1–6]. The modifications include rock softening, strength weakening, and degradation of the elastic modulus. Since the 1970s, numerous studies have been conducted to determine the effects of elevated temperatures on the physico-mechanical properties and deformation of granitic rocks [7–17]. However, most studies have concentrated on the changes to the samples after the sample had been heated [13, 18–27] rather than to follow the changes that take place during heating. Since heat restoring is of great significance to the next turn of heat extraction, the thermal crack damage process during heating should be considered. To monitor the thermal microcracking effect of temperature on crystalline rocks, some scholars employed various methods, such as direct wave velocity measurement, coda wave interferometry (CWI), permeability test and acoustic emissions (AE) to track the thermal cracking process during heating and thus reveal the thermal cracking mechanism [7, 16, 28, 29]. Hence, it is necessary to understand the failure response of granite under high temperature, particularly under high temperature that above 200°C. At

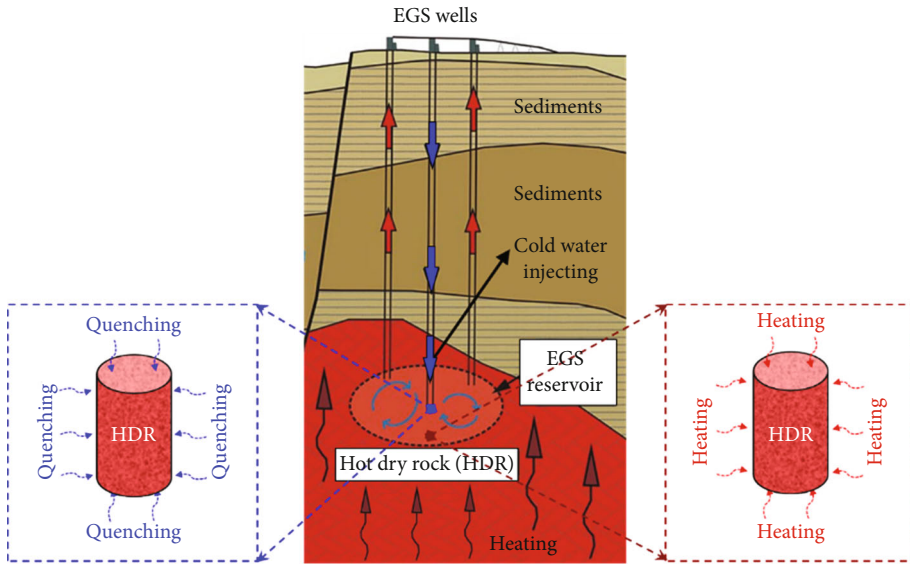

Figure 1: Heating and quenching of HDR in a typical EGS.

these temperatures, the properties of the rock are dramatically different than when they are at Earth-surface temperatures. In addition, understanding the HDR's performances during straightforward heating and quenching would be helpful to improve thermal treatment efficiency during EGS reservoir building.

Generally, higher temperatures result in a lower UCS and a reduced elastic modulus of brittle rock. However, the downward trends varies owing to the different compositions of the specimens tested and differences in experimental techniques. For the straightforward heating tests, cooling methods, such as quenching, cooling in air, or cooling in a furnace, can significantly affect the mechanical and physical properties of the specimen [19, 30]. In addition, both thermal cracking and the quartz α-β phase transition [31] can contribute to the dramatic changes. The uncertainties introduced by different cooling methods could be eliminated by conducting high-temperature tests.

The main mechanisms that weaken the granite are physical damages caused by thermal expansion and the thermal changes in rock minerals [32]. Specifically, spatial and temporal changes in temperature can induce microcracking as a result of differential thermal expansion between grains with different thermoelastic moduli and thermal conductivities. However, there are also other mechanisms involved like resistance to crack initiation and propagation under high temperatures (toughening mechanisms) [27]. By using computed tomography (micro-CT scans), Zhao and coworkers [16, 33] revealed that thermal cracks develop as the temperature increases. A few microfissures were observed at temperatures under 200°C. With increasing temperature, more microfissures were initiated and coalesced, leading to the development of new microcracks and the propagation of pre-existing cracks. To provide a link between the microstructural parameters and the mechanical behaviour of rock, Griffiths et al. [34] provided robust measurements of microcrack characteristics to constrain micromechanical models for rock strength and stiffness, which bridged the gap between the measurements of microcrack density at the microscale and the measurements of mechanical properties at the sample scale. During heating, a number of physical and mineralogical changes take place and these phenomena eventually result in thermal damage. The α-β quartz phase transformation occurs at 573°C and consequently, causing the volume of the quartz crystal to increase. This causes cracks in the rock resulting in weakened mechanical properties [20, 35–37]. These complex mineral thermal transitions are also important factors causing weakening and the brittle-ductile transition during deformation [38–40].

It is necessary to understand the real-time response of granite to deformation at high temperatures at both macro and micro scales. For this study, uniaxial compression tests on Luhui granite were conducted at temperatures ranging from 20°C to 500°C. This research focused on investigating: (1) the influence of high temperatures on the UCS, elastic modulus, and acoustic emissions (AE) from the Luhui granite; (2) the quenching effect and heating effect of hot dry rock. The following sections describe the experimental methods and then present and discuss the results. Finally, several important findings are set forth in the conclusion part.

2. Materials and Methods

2.1. Luhui Granite Sample Preparation. Samples of Luhui granite were collected from an open-pit quarry in Zoucheng city, Shandong province, China. The Luhui granite blocks were carefully selected to avoid fractures, discontinuities, and microcracks that would influence the test results. The granite block (Figure 2(a)) was cut into smaller blocks (200 mm ×200 mm ×120 mm) for further processing in the laboratory. These smaller blocks were cored to produce 50 mm diameter cylinders 100 mm long (Figure 2(b)). Both ends of the cylindrical samples were ground to ensure the ends of the cylinders were flat and parallel to each other

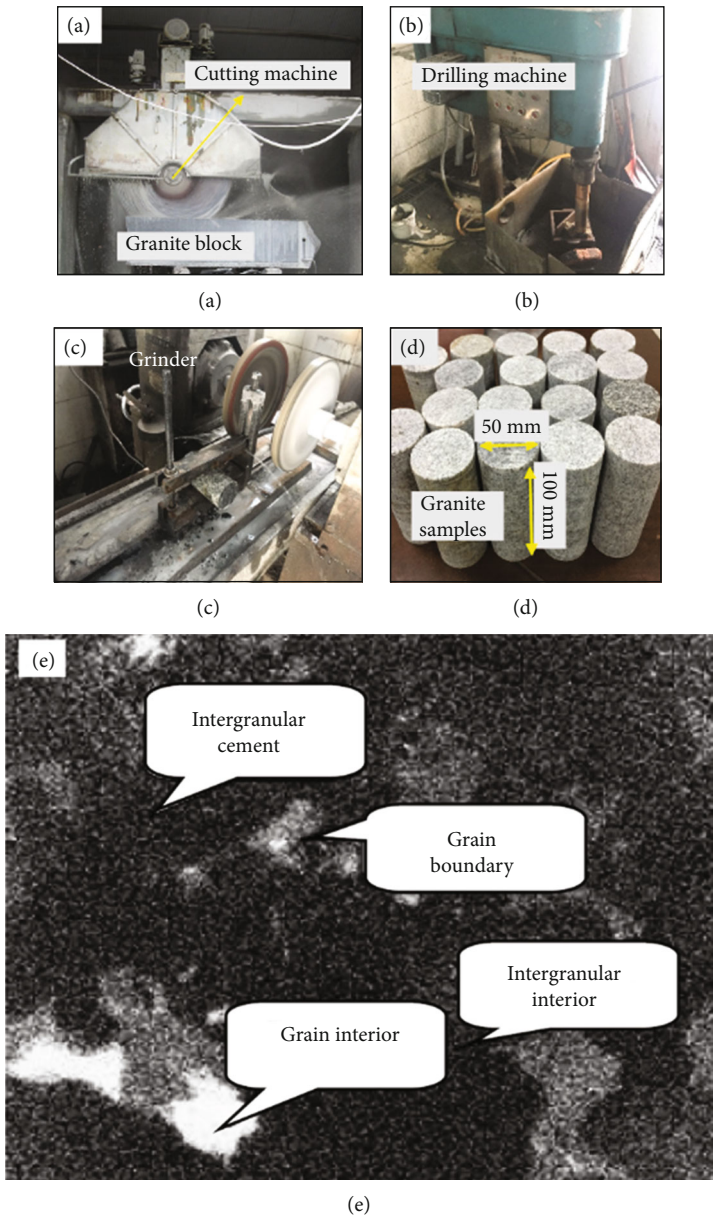

Figure 2: Photographs showing sample preparation and the meso-images of Luhui granite structure. (a) Rock saw cutting the granite block; (b) Core drill coring a smaller granite block; (c) Grinding the ends of a granite core; (d) Finished granite specimens 50 mm in diameter and 100 mm long; (e) Meso-image of Luhui granite structure at room temperature [7, 41].

(Figure 2(c)). Finished granite specimens are shown in Figure 2(d).

The Luhui granite is a strongly heterogeneous brittle and hard rock, mainly consist of feldspar, quartz, etc. Figure 2(e) shows the meso-structure of granite in the room temperature using high-accuracy micro-CT. Crystal grain, the boundary of grain, binding material among grain and grain pore can be clearly differentiated [41]. The main mineral compositions (feldspar, quartz) have almost the same proportion. However, the mechanical properties of these minerals differ greatly, making granites intensively heterogeneous.

2.2. Uniaxial Compression and Acoustic Emissions Test Procedures. The uniaxial compression experiments were carried out on a servo-controlled testing system with a maximum loading capacity of 300 kN and a displacement resolution of 0.001 mm. This servo-controlled system can test samples in either load (stress) or displacement (strain) control modes. In this test, the displacement (strain) control mode was employed. Specifically, the displacement rate for these tests on the Luhui granite specimens was set at 0.5 mm/min which equals to a strain rate of 8.33×10^{-5}/s.

To heat the samples, a temperature-controlled electric furnace was used to heat the samples to the target temperature at a heating rate of 4°C/min. The samples were held at the target temperature for two hours to achieve thermal equilibration and allow thermal reactions to proceed. For this study, the target temperatures were 20, 200, 300, 400, and

Table 1: The UCS and tangent modulus of granite under high temperatures.

Sample number	Temperature (°C)	UCS (MPa)	Average UCS (MPa)	Tangent modulus (GPa)	Average tangent modulus (GPa)
G-20C-1	20	86.7	116.0	18.0	13.6
G-20C-2		148.4		18.1	
G-20C-3		128.2		15.1	
G-20C-4		124.9		15.3	
G-20C-5		173.0		14.2	
G-20C-6		100.1		11.3	
G-20C-7		90.0		9.9	
G-20C-8		99.4		10.7	
G-20C-9		111.7		12.9	
G-20C-10		97.7		10.4	
G-200C-1	200	120.6	102.3	10.9	11.0
G-200C-2		111.5		11.7	
G-200C-3		84.3		10.1	
G-200C-4		92.7		11.2	
G-300C-1	300	72.1	84.5	9.4	10.0
G-300C-2		63.6		9.4	
G-300C-3		82.0		10.1	
G-300C-4		90.2		9.8	
G-300C-5		114.4		11.4	
G-400C-1	400	62.4	80.1	9.7	9.8
G-400C-2		99.9		10.8	
G-400C-3		78.4		8.9	
G-400C-4		79.7		9.8	
G-500C-1	500	80.8	79.7	9.0	9.8
G-500C-2		79.1		10.7	
G-500C-3		80.2		9.8	
G-500C-4		78.9		9.6	

500°C. Four uniaxial compression tests were run for each target temperature. Sample numbers and experimental conditions are listed in Table 1. To run a test, a cylindrical sample was placed in the center of the furnace and the piston applied compression to the ends of the sample after AE sensors were attached. Piston displacement and load were recorded simultaneously during the test as were the AE signals. It should be noted that AE sensors cannot be attached directly to the hot sample. Alternatively, these AE sensors were attached to the piston (Figure 3).

3. Results

3.1. Uniaxial Compression Results

3.1.1. Stress–Strain Curves for Granite Samples at High Temperatures. The uniaxial stress–strain curves for granite samples at different temperatures ranging from 20°C to 500°C are presented in Figure 4. The stress–strain curves for this brittle granite can be roughly divided into three stages, namely an original microcrack closure stage, an elastic deformation stage, and a final stage signaled by a sudden stress drop.

The first two stages, the microcrack closure and elastic deformation stages, occur before the maximum stress. During the microcrack closure (sealing) stage, the stress–strain curve is concave downward and this shape may result from the closure of primary pores and voids in the sample, although as pointed out by [42], some of the test conditions and imperfections in sample preparation can also contribute to the shape of the downward concave stress–strain curve. During the elastic deformation stage, axial stress increases and elastic deformation dominates the stress–strain curve. The stress–strain relationship remains linear despite the fact that there are some irreversible changes at this stage, such as crack initiation. The elastic deformation stage ends when peak strength is attained and the stage is followed by a sudden stress drop in stress. At the sudden stress drop stage, the stress decreases abruptly from the peak to essentially zero resulting in the stress–strain curve becoming a vertical line.

From Figure 4, it can be seen that the stress–strain curves are temperature dependent. Specifically, the peak strength and rigidity vary with the temperature. This is discussed in the following section.

3.1.2. Uniaxial Compressive Strength and Tangent Modulus

(1) Effect of temperature on UCS. Figure 5 presents a graph showing UCS for the granite samples versus temperature; the corresponding UCS and tangent modulus values are listed in Table 1. It can be seen that the average UCS value decreases with increasing temperature. The UCS-temperature curve can be divided into three sections by the UCS degradation rate. From 20°C to 200°C, the average UCS decreases from 112.7 MPa to 102.3 MPa. Thus, in this range the UCS decreases slightly with a UCS degradation rate of 0.058 MPa/°C. From 200°C to 300°C, the average UCS drop is more significant. In this range, the UCS value drops from 102.3 MPa to 84.5 MPa, in other words, the UCS degradation rate equals 0.178 MPa/°C. Above 300°C, the average UCS continues to decrease but the degradation rate is very low (only 0.024 MPa/°C). It appears that the thermal damage to the granite may be initiated between 20°C and 200°C, is enhanced between 200°C and 300°C, but little additional damage takes place above 300°C.

As shown in Figure 5, the UCS of the granite at 200–300°C is lower than that at room temperature. During the loading process, the thermal stresses enhance fissure expansion and stress softening. Therefore, the UCS decreases with increasing temperature. In addition, the changes in mineral composition and microcracking lead to degradation of the mechanical properties. In the aspect of data scattering, the large scattering in the UCS data at room temperature disappeared almost completely at 500°C. The large scattering at room temperature may be due to sample imperfections and the heterogeneity of rock. Granite is one of the crystalline rocks, which is mainly composed of quartz, feldspar and

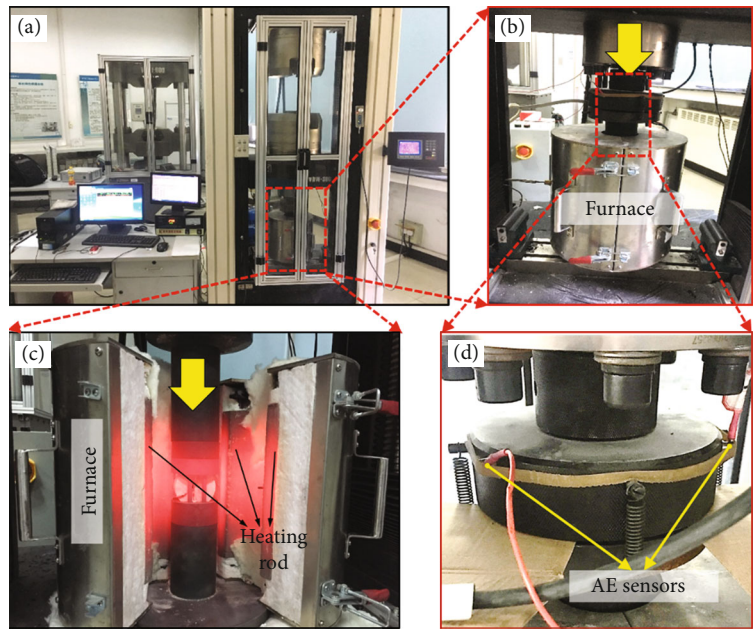

Figure 3: Photographs of the test systems showing the uniaxial compression test machine with the test control and data acquisition equipment (a), the furnace surrounding a sample (b and c) and a more detailed view of the acoustic emission sensors attached to the piston (d).

other minerals. During compression at room temperature, cracking is rather random, thus the strength was mostly controlled by the sample imperfections. However, the variations in UCS tend to be uniform at high temperatures, because more and more thermally induced microcracks controlled the strength of rock. That is to say, thermal cracking in rock, to some extent, could release the imperfection and the heterogeneity of rock.

(2) Effect of temperature on tangent modulus. The parameter of tangent modulus (E) represents the resistance of a sample during the stage of elastic compressing. On a stress–strain curve, the tangent modulus is defined as the slope of the elastic deformation portion of the curve. During the elastic deformation stage, the compressive stress increases linearly with the axial strain and elastic deformation dominates a stress–strain curve in the pre-peak region. The elastic moduli for the granite at different temperatures can be derived from the stress–strain curves; they are listed in Table 1 and plotted in Figure 6. The average tangent modulus of the granite decreases with increasing temperature. The curve in Figure 6 can be divided into two sections. In the temperature range 20–300°C, the tangent modulus decreases significantly from 13.6 GPa to 10.0 GPa, whereas at temperatures above 300°C, only a slight decrease, from 10.0 GPa to 9.8 GPa, occurs - the granite softens at high temperatures.

3.2. Acoustic Emission Results. Microcracking was monitored by counting dynamic rupture events in the granite samples using AE. Figure 7 shows typical stress–strain curves for each test temperature plotted on AE count vs. time axes for granite samples under the five different high-temperature test environments.

The microcracking activity shown in each of the panels on Figure 8 can clearly be divided into two periods, namely a quiescent period and an active period. During the quiescent period, there are few or no AE counts recorded. During the active AE period, the stress–strain curve reflects two different types of deformation, a stage of elastic deformation and a stage of crack growth and propagation. In the elastic deformation stage, there are one or more stress drops that may represent microfracture propagation. This fracturing is not in all cases evident in the stress–strain curves but is detected by the AE sensors and is manifested by a sudden increase in AE counts.

The intensity of the microcracking in the granite samples changes with temperature. As shown in Figure 8, the number of AE counts decreases and counts are recorded less frequently at higher temperatures indicating that the granite becomes much more ductile at high temperatures. This result is consistent with the lower tangent modulus at these temperatures. Interestingly, the cumulative AE count versus time curves show distinct steps at the higher temperatures indicating several failures in the samples. These failures will be discussed in the following sections on failure modes and grain size distributions.

4. Discussion

4.1. Thermal Micro-Cracking Effect of Granite. Zhai et al. [43] investigated thermal effects on the strength of granite from the aspect of energy storage and release. A higher temperature implies greater thermal energy in the granite, and this can result in a larger energy releases when fissures coalesce and propagate before failure. After completing a study on thermal cracking, Zhao and coworkers [16] reported that

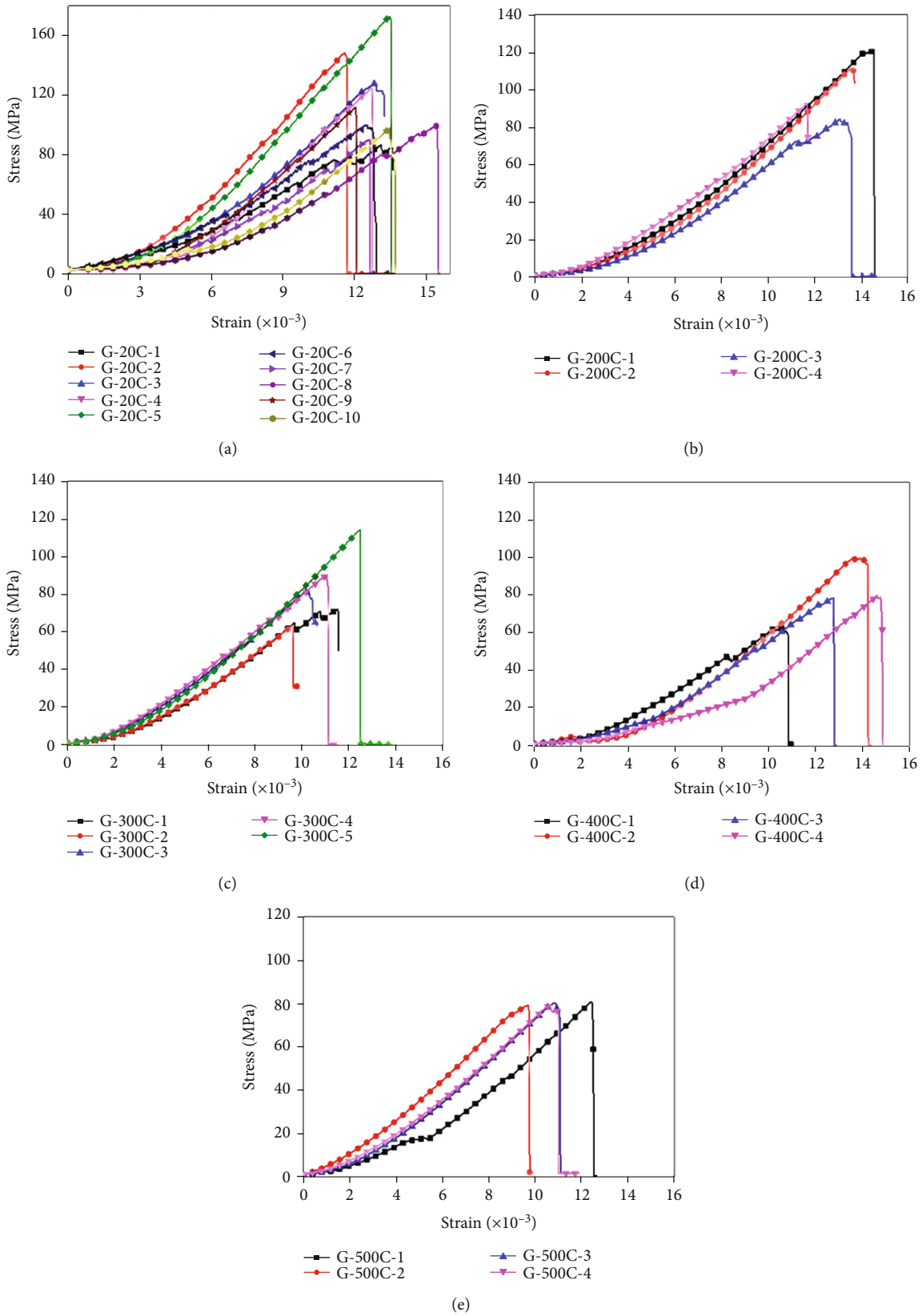

Figure 4: Uniaxial stress versus strain curves for granite at different temperatures. (a) room temperature (~20°C); (b) 200°C; (c) 300°C; (d) 400°C; (e) 500°C.

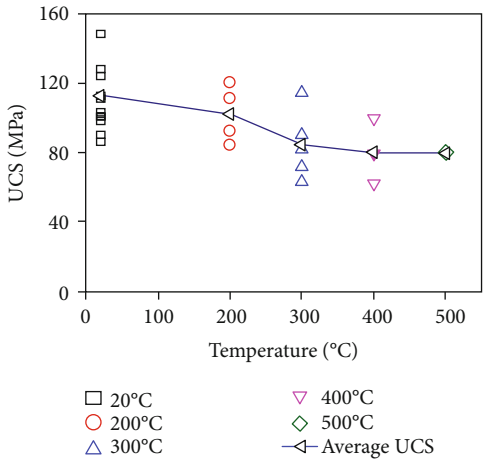

Figure 5: Uniaxial compressive strength of the granite samples vs. temperature.

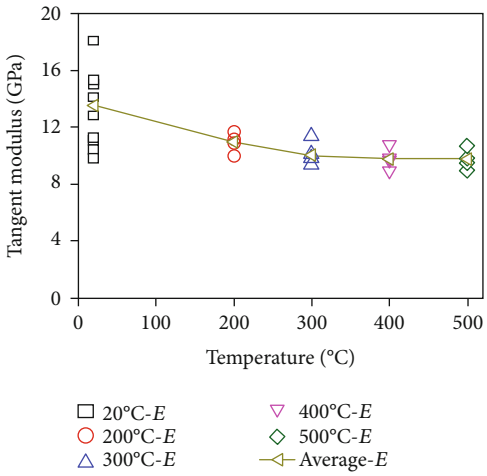

Figure 6: Effect of temperature on the tangent modulus of granite samples.

thermal fracturing in the Luhui granite increased at higher temperatures. Figure 7(a) shows the CT images of the meso-structure of Luhui granite specimens under different temperatures (20°C, 200°C, 300°C and 500°C). There are no obvious micro-cracks at room temperature. A few micro-fractures were observed at temperatures below 200°C. The crystal particles are surrounded by a large majority of micro-cracks in weakening lines when heated to 200°C. But a large-closed polygon crack around granitic particles has not yet been formed. Large cracks can be observed, and the crack length increased significantly when heating to 300°C. Specifically, the length of a fissure in the granite could be 10 times longer at 300°C than a fissure at 200°C, which would significant destroy the tight and intact structure of rock and thus weaken its strength. Importantly, when the temperature increased to 500°C, the crystal grains in the granite were almost surrounded by micro-fractures. More than 90% of the micro-fractures (either boundary or cleavage cracks [17, 26, 44]) occurred on the boundaries of rock grains, although minor transgranular cracks [45, 46] cut across mineral grains. In addition, Yang et al. [26] indicated that mineral grains in granites are closely arranged and linked. At 400–600°C, the boundary cracks and transgranular cracks in the feldspar and quartz grains would diminish the strength and stiffness of the rock. The knowledge that thermal cracking generates these cracks and fissures suggests that, after failure, the grain sizes of the failure fragments would be smaller.

By conducting MPV micro-photometer test, Feng et al. [7] revealed the micro-crack quantity change with temperature in thermally cracked Luhui granite. As shown in Figure 7(b), for the quantity of micro-crack curve (Length>5 μm), there are two peaks and the corresponding temperature are 100–150°C and 250–300°C, respectively. The second peak of micro-crack quantity occurs at around 300°C which is larger than the first peak. The explanation of thermally induced micro-crack occurrence is inharmonious thermal expansion, which can result in thermal stress in granite. When the temperature in granite increased to 100–150°C, thermal stress among the majority of mineral grains may exceed bonding stress and intergranular micro-cracks largely occur. The quantity peak of Length>5 μm micro-cracks thus occurs. When the temperature increased further to 250–300°C, thermal stress may exceed inner bonding stress in mineral crystal and transgranular microcracks largely happen, which causes a second large increment of microcracks. The quantity of micro-crack whose length is greater than 10 μm (Length>10 μm) has the same evolution. The temperature of quantity increasing of Length>10 μm micro-crack corresponds to that of Length>5 μm micro-crack quantity reduction. It can illustrate that small micro-cracks propagate and interconnect each other to form large micro-crack after small micro-crack initiating with the temperature rising. These results are consistent with the CT image results shown in Figure 7(a). These findings can explain why the UCS changes with temperature, especially the sharp UCS drop at 200-300°C.

4.2. Comparison of Rock's Mechanical Property between Straightforward Heating and Quenching Treatments. In EGS system, injecting cold water into HDR occurs a lot for thermal stimulation [47–50]. As above mentioned, the increase of temperature may reduce the compressive strength, tangent modulus and other mechanical parameters of HDR to a certain degree. During quenching, both strength and elastic properties of granite could significantly decrease due to the intense thermal shock which creates considerable thermal damage to the rock structure. Therefore, it is necessary to understand how does the mechanical property changes in straightforward heating and quenching conditions.

Xi and Zhao conducted the quenching tests of Luhui granite from room temperature to 500°C. After heating the Luhui granite samples [23], cold water was utilized to quench these samples and the UCS values were obtained afterwards. Figure 9(a) presents the variation of UCS values versus the temperature and Figure 9(b) shows the normalized USC-temperature curve. Black lines show our high-temperature test results, while the dotted lines are quenched test results. Noted that the normalized UCS is the ratio between the UCS value at various temperatures and the UCS value that gained at room temperature. Similarly, Figures 9(c) and 9(d) present the relationship between the actual tangent

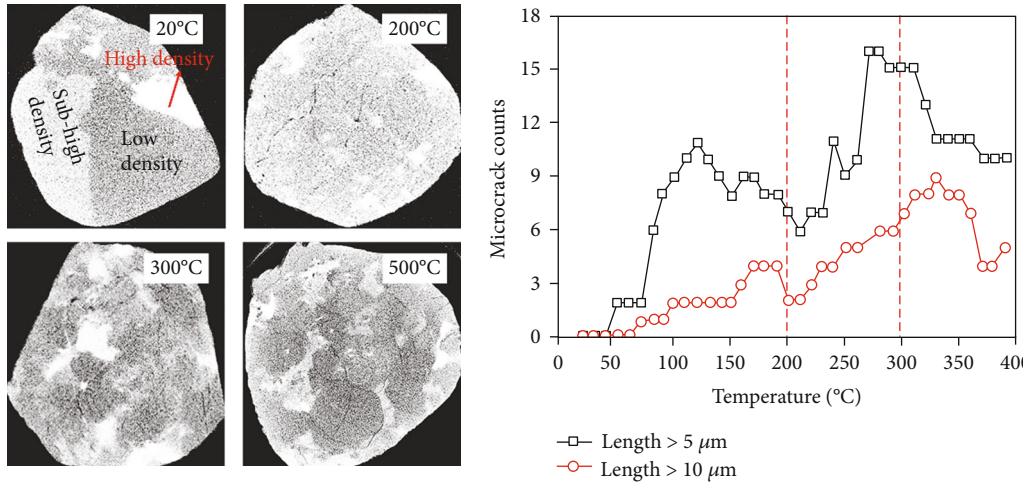

(a) (b)

Figure 7: CT images of meso-structure during thermal cracking of Luhui granite specimen (modified from Zhao et al. [16]) (a); Variation in the quantity of micro-crack of Luhui granite (modified from Feng et al. [7]) (b).

modulus values as well as the normalized tangent modulus and the temperature, respectively.

The UCS values of Luhui granite at room temperature varies because of the difference of sampling locations and weathering conditions of rock specimen, for instance, the UCS value of Luhui granite that we obtained is 116 MPa, which differs from Xi and Zhao's result [23]. However, the tendency of UCS variation with temperatures is consistent. Three sections are observed from the UCS vs temperature curves. Section I: UCS values decrease slightly at the temperature range of 20-200°C. Section II: UCS values decreases sharply from 200 to 300°C. Section III: The decreasing rate of UCS stabilizes from 300 to 500°C. Specifically, the strength of rock would be further quenching weakened by 10%, 20% and 30% at 200°C, 300°C and 500°C, respectively. Apart from the UCS values, the relationship between the tangent modulus of the Luhui granite specimens and the temperature is also obtained. It was found that the tangent modulus decreases with the temperature for both straightforward heated and quenched granite specimens (Figures 9(c) and 9(d)).

In addition, the normalized UCS and tangent modulus values obtained from the quenching test are smaller than those values that gained from the high-temperature conditions. Furthermore, the quenched normalized curves decrease faster than that of high-temperature curves, meaning that quenching or injecting cold water into HDR would further weaken the rock and creates thermal damage to the rock structure.

Granite is one of the crystalline rocks. In the heterogeneous rock, thermal cracking is rather random. The main reason for thermally induced micro-crack occurrence is inharmonious thermal expansion of mineral grains, which can result in thermal stress in granite. Temperature change (i.e. thermal gradient) is the main factor that induces thermal stress. Specifically, a larger temperature change always implies a higher thermal stress. Once local thermal stress exceeds the binding stress among the same/different constituted particles, thermal cracking would occur and thus result in micro-crack initiation, propagation and interconnection. Therefore, quenching (with a sharp temperature change) induced rock damage is much more destructive than normal temperature rising.

5. Implications of Geothermal Mining in HDR by EGS

The temperature variation may induce the change of mechanical parameters and may result in the thermal shock to the granite specimens [23, 51, 52]. The temperature has a great influence on the mechanical parameters of granite, which is mainly reflected in the tangent modulus, compressive strength, etc..

As shown in Figure 1, the concept of EGS is to exploit geothermal resources from the earth by drilling wells into HDR. A well is drilled first to inject cold water at high pressure to stimulate or hydraulically fracturing the natural rock joints, thereby creating a geothermal reservoir. Injected cold water picks up heat and returns to the surface via the production well. In the process injecting cold water to HDR, the rock would rapidly be cooled at a high rate, inevitably leading to the thermal shock within the reservoir rock. Because of the rapid cooling, a relatively higher thermal gradient will be generated compared to that from the steady heat flow. This higher thermal gradient will certainly generate a greater thermal stress component.

This study investigated the failure response of granite specimen, and discussed the difference of rock mechanical properties between straightforward heating and quenching treatments. Macroscopic failure rock is always caused by micro-crack initiation, propagation, interconnection etc. Fracture in rocks under compressive boundary loads is a result of the coalescence of many microcracks, not the growth of a single crack [17]. As compression stress increases and rock failure is approached, the microcrack population changes spatially from random to locally intense zones of cracking. High thermal treatment on an impermeable rock, such as quenching, is likely to create new thermal cracks. The implication of HDR is that when wells are drilled into

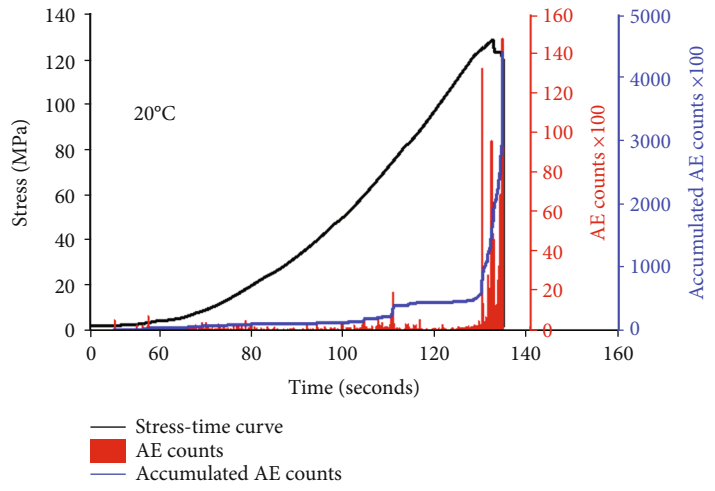

(a)

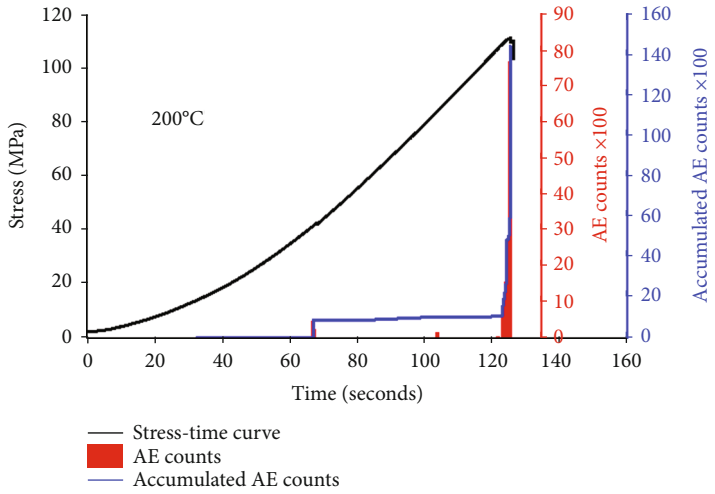

(b)

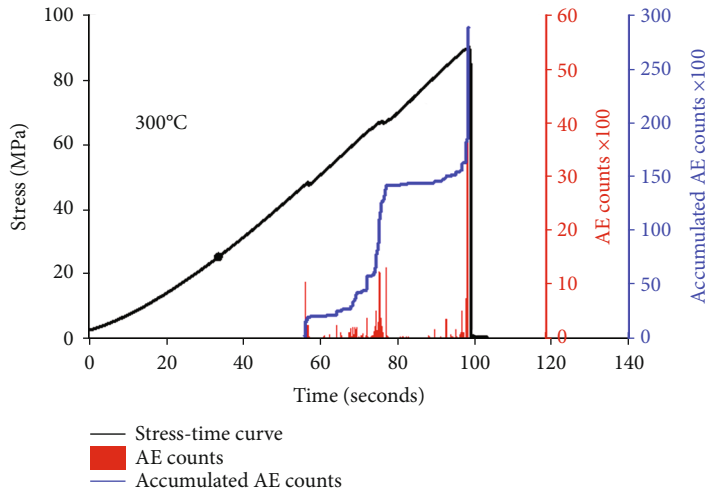

(c)

Figure 8: Continued.

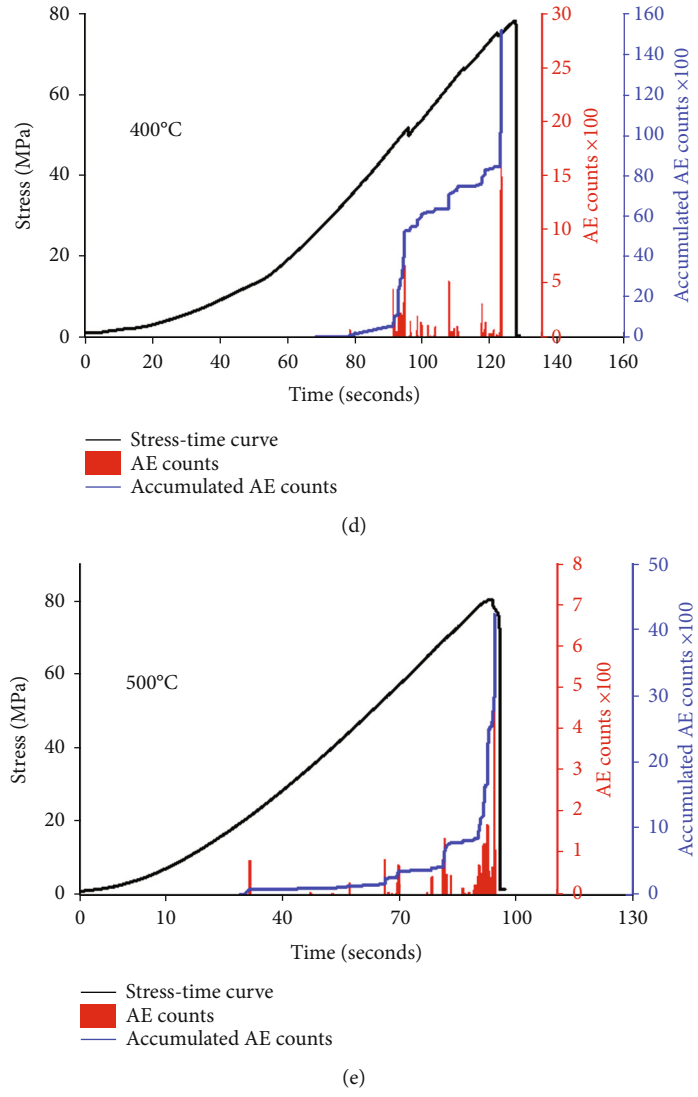

Figure 8: Typical stress–strain curves and acoustic emission counts for granite samples at high temperatures. (a) 20°C; (b) 200°C; (c) 300°C; (d) 400°C; (e) 500°C.

high-temperature rocks, but with poor flow circulation because of lacking flow path, thermal cracking processes could be a worthwhile pursuit to enhance the permeability. Therefore, in the process of geothermal reservoir stimulation and enhancement, rock failure response under heating and quenching treatments cannot be ignored. During drilling, injecting, hydraulic fracturing and hydroshearing [53, 54], rock failure response and the mechanisms due to the temperature variation should be fully utilized to improve well drilling and reservoir building efficiency.

6. Conclusions

Understanding the influence of temperature on granite failure is of great interest to engineers involved with enhanced geothermal energy systems and nuclear waste disposal projects. In this study, the mechanical behavior and deformation of granite at high temperatures ranging from 20°C to 500°C were systematically studied at both macro to micro scales. Several conclusions can be drawn.

(1) Both the uniaxial compressive strength (UCS) and tangent modulus decrease with increasing temperature. The UCS–temperature curve can be divided into three sections: the UCS decreases slightly between 20°C and 200°C, significantly between 200°C and 300°C, and then the rate of decrease slows drastically in the interval 300°C to 500°C. However, as the temperature increases from 20°C to 500°C, the tangent modulus decreases exponentially.

(2) The number of acoustic emission (AE) counts recorded also changes with temperature. At higher temperatures, the number of AE counts decreases and counts are recorded less frequently. This indicates that the granite becomes much more ductile at high temperatures.

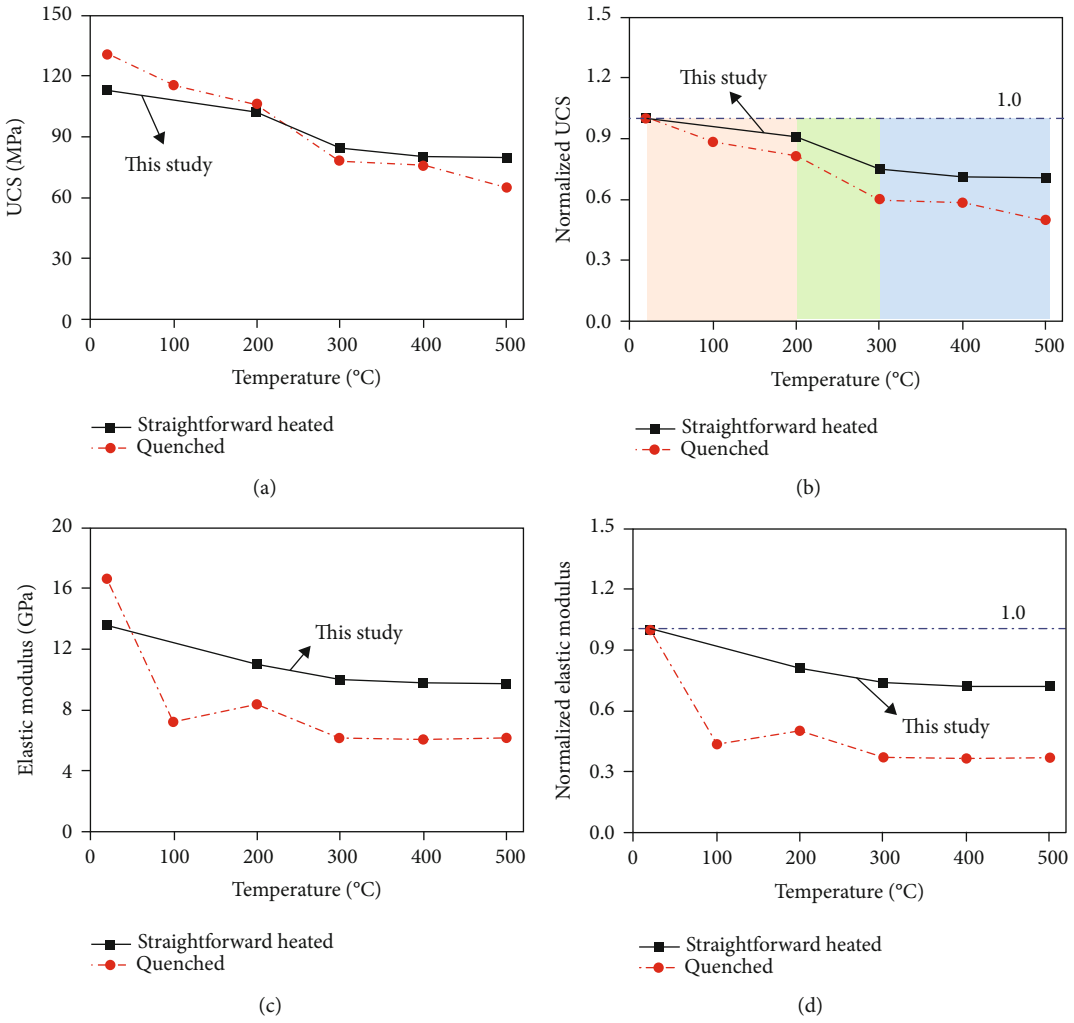

Figure 9: UCS and elastic modules of granite under different thermal treatments. (a) UCS versus temperature curves; (b) Normalized UCS versus temperature curves; (c) Tangent modulus versus temperature curves; (d) Normalized tangent modulus versus temperature curves.

(3) Quenching or injecting cold water into HDR would further weaken the rock and create thermal damage to the rock structure. The strength of rock would be further quench-weakened by 10%, 20% and 30% at 200°C, 300°C and 500°C, respectively. Therefore, in EGS systems, quenching is much more destructive than the application of normal thermal stresses, which could be fully utilized to improve well drilling and reservoir stimulation.

Data Availability

The data used to support the findings of this study are available from the corresponding author upon request.

Additional Points

Highlights. (1) Both the uniaxial compression strength (UCS) and tangent modulus of granite decrease with increasing temperature. (2) The UCS-temperature curve follows a three-stage strain-dependent evolution. (3) Quenching is much more destructive than normal thermal stress.

Conflicts of Interest

The authors declare that there is no conflict of interest regarding the publication of this paper.

Acknowledgments

This work was supported by the Fundamental Research Funds for the Central Universities (2020XJNY03 and 2017XKZD06) and the YueQi Distinguished Scholar Project of China University of Mining & Technology, Beijing.

References

[1] R. G. S. Araújo, J. L. A. O. Sousa, and M. Bloch, "Experimental investigation on the influence of temperature on the mechanical properties of reservoir rocks," *International Journal of Rock Mechanics & Mining Sciences*, vol. 34, no. 3–4, pp. 298.e1–298.16, 1997.

[2] S. J. Bauer and J. Handin, "Thermal expansion and cracking of three confined water-saturated igneous rocks to 800°C," *Rock Mechanics & Rock Engineering*, vol. 16, no. 3, pp. 181–198, 1983.

[3] R. D. Dwivedi, R. K. Goel, V. V. R. Prasad, and A. Sinha, "Thermo-mechanical properties of Indian and other granites," *International Journal of Rock Mechanics & Mining Sciences*, vol. 45, no. 3, pp. 303–315, 2008.

[4] Y. Mahmutoglu, "Mechanical behaviour of cyclically heated fine grained rock," *Rock Mechanics & Rock Engineering*, vol. 31, no. 3, pp. 169–179, 1998.

[5] J. Fan, P. Liu, J. Li, and D. Jiang, "A coupled methane/air flow model for coal gas drainage: model development and finite-difference solution," *Process Safety and Environmental Protection*, vol. 141, pp. 288–304, 2020.

[6] A. Liu, S. Liu, X. Hou, and P. Liu, "Transient gas diffusivity evaluation and modeling for methane and helium in coal," *International Journal of Heat and Mass Transfer*, vol. 159, article 120091, 2020.

[7] Z. Feng, Y. Zhao, Y. Zhang, and Z. Wan, "Real-time permeability evolution of thermally cracked granite at triaxial stresses," *Applied Thermal Engineering*, vol. 133, pp. 194–200, 2018.

[8] C. Goetze, "High temperature rhelogy of westerly granite," *Journal of Geophysical Research*, vol. 76, no. 5, pp. 1223–1230, 1971.

[9] F. E. Heuze, "High-temperature mechanical, physical and Thermal properties of granitic rocks– A review," *International Journal of Rock Mechanics & Mining Sciences & Geomechanics Abstracts*, vol. 20, no. 1, pp. 3–10, 1983.

[10] S. Kou, "Effect of thermal cracking damage on the deformation and failure of granite," *Acta Mechanica Sinica*, vol. 242, pp. 235–240, 1987.

[11] S. Liu and J. Xu, "An experimental study on the physico-mechanical properties of two post-high- temperature rocks," *Engineering Geology*, vol. 185, no. 4, pp. 63–70, 2015.

[12] I. van der Molen, "The shift of the α-β transition temperature of quartz associated with the thermal expansion of granite at high pressure," *Tectonophysics*, vol. 73, no. 4, pp. 323–342, 1981.

[13] Q. Sun, W. Zhang, L. Xue, Z. Zhang, and T. Su, "Thermal damage pattern and thresholds of granite," *Environmental Earth Sciences*, vol. 74, no. 3, pp. 2341–2349, 2015.

[14] Z. Wan, Y. Zhao, F. Dong, Z. Feng, N. Zhang, and J. Wu, "Experimental study on mechanical characteristics of granite under high temperatures and triaxial stresses," *Chinese Journal of Rock Mechanics & Engineering*, vol. 27, no. 1, pp. 72–77, 2008.

[15] T. F. Wong, "Effects of temperature and pressure on failure and post-failure behavior of westerly granite," *Mechanics of Materials*, vol. 1, no. 1, pp. 3–17, 1982.

[16] Y. S. Zhao, Z. J. Wan, Z. J. Feng, Z. H. Xu, and W. G. Liang, "Evolution of mechanical properties of granite at high temperature and high pressure," *Geomechanics and Geophysics for Geo-Energy and Geo-Resources*, vol. 3, no. 2, pp. 199–210, 2017.

[17] R. L. Kranz, "Microcracks in rocks: a review," *Tectonophysics*, vol. 100, no. 1-3, pp. 449–480, 1983.

[18] X. Xu, Z. Kang, M. Ji, W. Ge, and J. Chen, "Research of microcosmic mechanism of brittle-plastic transition for granite under high temperature," *Procedia Earth & Planetary Science*, vol. 1, no. 1, pp. 432–437, 2009.

[19] H. Zhu, Z. Yan, T. Deng, J. Yao, L. Zeng, and J. Qiang, "Testing study on mechanical properties of tuff, granite and breccia after high temperatures," *Chinese Journal of Rock Mechanics & Engineering*, vol. 25, no. 10, pp. 1945–1950, 2006.

[20] S. Yin, R. Shu, X. Li, P. Wang, and X. Liu, "Comparison of mechanical properties in high temperature and thermal treatment granite," *Transactions of Nonferrous Metals Society of China*, vol. 26, no. 7, pp. 1926–1937, 2016.

[21] L. P. Zhi, J. Y. Xu, J. Z. Jin, S. Liu, and T. F. Chen, "Research on ultrasonic characteristics and mechanical properties of granite under post-high temperature," *Chinese Journal of Underground Space and Engineering*, vol. 8, no. 4, pp. 54–59, 2012.

[22] Y. Chen, W. Shao, and Y. Zhou, "Experimental study on mechanical properties of granite after high temperature," *Chinese Quarterly of Mechanics*, vol. 32, no. 3, pp. 397–402, 2011.

[23] B. Xi and Y. Zhao, "Experimental research on mechanical properties of water-cooled granite under high temperatures within 600°C," *Chinese Journal of Rock Mechanics & Engineering*, vol. 29, no. 5, pp. 892–898, 2010.

[24] S. J. Du, H. Liu, H. T. Zhi, and H. H. Chen, "Testing study on mechanical properties of post-high-tempearture granite," *Chinese Journal of Rock Mechanics & Engineering*, vol. 23, no. 14, pp. 2359–2364, 2004.

[25] Y. L. Chen, S. R. Wang, J. Ni, R. Azzam, and T. M. Fernández-steeger, "An experimental study of the mechanical properties of granite after high temperature exposure based on mineral characteristics," *Engineering Geology*, vol. 220, pp. 234–242, 2017.

[26] S. Q. Yang, P. G. Ranjith, H. W. Jing, W. L. Tian, and Y. Ju, "An experimental investigation on thermal damage and failure mechanical behavior of granite after exposure to different high temperature treatments," *Geothermics*, vol. 65, pp. 180–197, 2017.

[27] G. M. N. Rao and C. R. Murthy, "Dual role of microcracks: toughening and degradation," *Canadian Geotechnical Journal*, vol. 38, no. 2, pp. 427–440, 2001.

[28] L. Griffiths, O. Lengliné, M. J. Heap, P. Baud, and J. Schmittbuhl, "Thermal cracking in westerly granite monitored using direct wave velocity, coda wave interferometry and acoustic emissions," *Journal of Geophysical Research Solid Earth*, vol. 123, no. 3, pp. 2246–2261, 2018.

[29] J. Browning, P. Meredith, and A. Gudmundsson, "Cooling-dominated cracking in thermally stressed volcanic rocks," *Geophysical Research Letters*, vol. 43, no. 16, pp. 8417–8425, 2016.

[30] K. Kim, J. Kemeny, and M. Nickerson, "Effect of rapid thermal cooling on mechanical rock properties," *Rock Mechanics & Rock Engineering*, vol. 47, no. 6, pp. 2005–2019, 2014.

[31] C. V. Raman and T. M. K. Nedungadi, "The α-β transformation of quartz," *Nature*, vol. 145, no. 3665, pp. 147–1912, 1940.

[32] Y. Chen, D. Li, Q. Jiang, and C. Zhou, "Micromechanical analysis of anisotropic damage and its influence on effective thermal conductivity in brittle rocks," *International Journal of Rock Mechanics & Mining Sciences*, vol. 50, no. 2, pp. 102–116, 2012.

[33] Y. Zhao, Q. Meng, T. Kang, N. Zhang, and B. Xi, "Micro-ct experimental technology and meso-investigation on thermal fracturing characteristics of granite," *Chinese Journal of Rock Mechanics & Engineering*, vol. 27, no. 1, pp. 28–34, 2008.

[34] L. Griffiths, M. J. Heap, P. Baud, and J. Schmittbuhl, "Quantification of microcrack characteristics and implications for stiffness and strength of granite," *International Journal of Rock Mechanics Mining Sciences*, vol. 100, pp. 138–150, 2017.

[35] G. Dolino and J. P. Bachheimer, "Fundamental and second-harmonic light scattering by the α-β coexistence state of quartz," *Physica Status Solidi*, vol. 41, no. 2, pp. 673–677, 2010.

[36] S. Kume and N. Kato, "A furnace for high-temperature X-ray diffraction topography," *Journal of Applied Crystallography*, vol. 7, no. 4, pp. 427–429, 2010.

[37] C. M. E. Zeyen, G. Dolino, and J. P. Bachheimer, "Neutron and calorimetric observation of a modulated structure in quartz just above the α-β phase transition," *Physica B+C*, vol. 120, no. 1-3, pp. 280–282, 1983.

[38] J. T. Fredrich and T. Wong, "Micromechanics of thermally induced cracking in three crustal rocks," *Journal of Geophysical Research Solid Earth*, vol. 91, no. B12, pp. 12743–12764, 1986.

[39] Z. Zhang, F. Gao, and X. Xu, "Experimental study of temperature effect of mechanical properties of granite," *Rock and Soil Mechanics*, vol. 32, no. 8, pp. 2346–2352, 2011.

[40] S. Shao, P. G. Ranjith, P. L. P. Wasantha, and B. K. Chen, "Experimental and numerical studies on the mechanical behaviour of Australian Strathbogie granite at high temperatures: an application to geothermal energy," *Geothermics*, vol. 54, no. 54, pp. 96–108, 2015.

[41] Y. Zhao, Z. Feng, Y. Zhao, and Z. Wan, "Experimental investigation on thermal cracking, permeability under HTHP and application for geothermal mining of HDR," *Energy*, vol. 132, pp. 305–314, 2017.

[42] A. Korinets and H. Alehossein, "Technical note on the initial non-linearity of compressive stress-strain curves for intact rock," *Rock Mechanics & Rock Engineering*, vol. 35, no. 4, pp. 319–328, 2002.

[43] S. Zhai, G. Wu, Y. Zhang, C. Luo, and Y. Li, "Research on acoustic emission characteristics of granite under high temperature," *Chinese Journal of Rock Mechanics & Engineering*, vol. 32, no. 1, pp. 126–134, 2013.

[44] M. Sarfarazi and S. K. Ghosh, "On the micromechanical theories of stressinduced cleavage microcracking in crystalline solids," *Engineering Fracture Mechanics*, vol. 27, no. 2, pp. 215–230, 1987.

[45] V. M. Goritskii, "A criterion of failure of steels susceptible to propagation of brittle microcracks along crystal boundaries," *Strength of Materials*, vol. 19, no. 4, pp. 479–486, 1987.

[46] B. Obara, "Identification of transcrystalline microcracks observed in microscope images of a dolomite structure using image analysis methods based on linear structuring element processing," *Computers & Geosciences*, vol. 33, no. 2, pp. 151–158, 2007.

[47] P. A. Siratovich, M. C. Villeneuve, J. W. Cole, B. M. Kennedy, and F. Bégué, "Saturated heating and quenching of three crustal rocks and implications for thermal stimulation of permeability in geothermal reservoirs," *International Journal of Rock Mechanics Mining Sciences*, vol. 80, pp. 265–280, 2015.

[48] A. Ghassemi, "A review of some rock mechanics issues in geothermal reservoir development," *Geotechnical Geological Engineering*, vol. 30, no. 3, pp. 647–664, 2012.

[49] G. Izadi and D. Elsworth, "Reservoir stimulation and induced seismicity: roles of fluid pressure and thermal transients on reactivated fractured networks," *Geothermics*, vol. 51, pp. 368–379, 2014.

[50] J. Taron and D. Elsworth, "Thermal-hydrologic-mechanical-chemical processes in the evolution of engineered geothermal reservoirs," *International Journal of Rock Mechanics Mining Sciences*, vol. 46, no. 5, pp. 855–864, 2009.

[51] C. Zhou, Z. Wan, Y. Zhang, and B. Gu, "Experimental study on hydraulic fracturing of granite under thermal shock," *Geothermics*, vol. 71, pp. 146–155, 2018.

[52] W. G. P. Kumari, P. G. Ranjith, M. S. A. Perera, and B. K. Chen, "Experimental investigation of quenching effect on mechanical, microstructural and flow characteristics of reservoir rocks: thermal stimulation method for geothermal energy extraction," *Journal of Petroleum Science Engineering*, vol. 162, pp. 419–433, 2018.

[53] A. P. Rinaldi and J. Rutqvist, "Joint opening or hydroshearing? Analyzing a fracture zone stimulation at Fenton Hill," *Geothermics*, vol. 77, pp. 83–98, 2019.

[54] Q. Yin, H. Jing, G. Ma, H. Su, and R. Liu, "Investigating the roles of included angle and loading condition on the critical hydraulic gradient of real rock fracture networks," *Rock Mechanics Rock Engineering*, vol. 51, no. 10, pp. 3167–3177, 2018.